# From Hope to Heuristic: Realistic Runtime Estimates for Quantum Optimisation in NHEP

*Maja* Franz[1,*], *Manuel* Schönberger[1], *Melvin* Strobl[2,**], *Eileen* Kühn[2], *Achim* Streit[2], *Pía* Zurita[3], *Markus* Diefenthaler[4], and *Wolfgang* Mauerer[1,5]

[1]Technical University of Applied Sciences Regensburg, Germany
[2]Karlsruhe Institute of Technology, Germany
[3]Complutense University of Madrid, Spain
[4]Jefferson Lab, VA, USA
[5]Siemens AG, Technology, Munich, Germany

**Abstract.** Noisy Intermediate-Scale Quantum (NISQ) computers, despite their limitations, present opportunities for near-term quantum advantages in Nuclear and High-Energy Physics (NHEP) when paired with specially designed quantum algorithms and processing units. This study focuses on core algorithms that solve optimization problems through the quadratic Ising or Quadratic Unconstrained Binary Optimisation model, specifically Quantum Annealing and the Quantum Approximate Optimisation Algorithm (QAOA).

In particular, we estimate runtimes and scalability for the task of particle Track Reconstruction (TR), a key computing challenge in NHEP, and investigate how the classical parameter space in QAOA, along with techniques like a Fourier-analysis based heuristic, can facilitate future quantum advantages. The findings indicate that lower frequency components in the parameter space are crucial for effective annealing schedules, suggesting that heuristics can improve resource efficiency while achieving near-optimal results. Overall, the study highlights the potential of NISQ computers in NHEP and the significance of co-design approaches and heuristic techniques in overcoming challenges in quantum algorithms.

## 1 Introduction

Noisy Intermediate-Scale Quantum (NISQ) computers, while limited by imperfections and small scale, hold promise for near-term quantum advantages in Nuclear and High-Energy Physics (NHEP) when coupled with co-designed quantum algorithms and special-purpose quantum processing units [1]. Developing co-design approaches is essential for near-term usability, but inherent challenges exist due to the fundamental properties of NISQ algorithms [2]. In this contribution we therefore investigate the core algorithms, which can solve optimisation problems via the abstraction layer of a quadratic Ising model or general Quadratic Unconstrained Binary Optimisation (QUBO), namely Quantum Annealing (QA) and the Quantum Approximate Optimisation Algorithm (QAOA). As an example for a variety of applications in NHEP utilising QUBO formulations [3], we focus on Track Reconstruction (TR) [4, 5]. TR

---

*e-mail: maja.franz@othr.de
**e-mail: melvin.strobl@kit.edu

is a good example of pattern recognition and optimisation in NHEP, and with TrackML [6], there exist curated datasets for algorithmic development along well-documented performance metrics. While QA and QAOA do not inherently imply quantum advantage, QA runtime for specific problems can be determined based on the physical properties of the underlying Hamiltonian, although it is a computationally hard problem itself [7]. Our primary focus is on two key areas: Firstly, we estimate runtimes and scalability for the common NHEP problem of TR addressed via a QUBO formulation [8]. This analysis is conducted by identifying minimum energy solutions of intermediate Hamiltonian operators encountered during the annealing process. Secondly, we investigate how the classical parameter space in the QAOA, together with approximation techniques such as a Fourier-analysis based heuristic, proposed by Zhou *et al.* [9], can help to achieve (future) quantum advantage, considering a trade-off between computational complexity and solution quality.

The remainder of this article is structured as follows: In Sec. 2 we provide a brief introduction to QA and explain how annealing schedules and energy levels link to Spectral Gaps (SGs). Sec. 3 then introduces QAOA, how it can be used to derive annealing schedules, and what heuristics exist for doing so. In Sec. 4, we briefly introduce the task of TR and describe our experimental setup with the results in Sec. 5. Finally, we conclude in Sec. 6. We ensure reproducibility [10], by providing the code as well as the numerical results that we use in the figures of this work in Ref. [11]. Notably, our experiments are performed using classical simulations of QAOA and QA with Qiskit [12].

## 2 Quantum Annealing

QA is, roughly speaking, a restricted version of adiabatic quantum computing [7] which is used to find minimum energy solutions to a problem (cost) Hamiltonian $\hat{H}_C$. The solutions are obtained by an adiabatic transition from a system, prepared in the ground state of an initial Hamiltonian $\hat{H}_0$, to $\hat{H}_C$. QA is restricted to a certain subclass of all possible Hamiltonians [7], which are equivalent to QUBO problems, to which any **NP** problem can be reduced [13]. The overall time-dependent Hamiltonian of the annealing process is determined by the "protocol" $f(t)$ that guides the transition between the Hamiltonians via

$$\hat{H}_{QA}(t) = -\left( f(t)\hat{H}_C + (1 - f(t))\hat{H}_0 \right) \tag{1}$$

By default, D-Wave annealers [14] implement a linear transition given by $f(t) = s := t/T$, where $T$ is the chosen *annealing time*, and $t \in [0, T]$. It is known that the minimum time $T_{\min}$ required for an adiabatic transition depends on the spectrum of the Hamiltonian $\hat{H}_{QA}$, in particular the minimum energy gap (SG $\Delta_{\min}$) between ground state and first excited state encountered when running the protocol given in Eq. 1 by $T_{\min} = O(1/\Delta_{\min}^2)$. Harder problems with longer required runtimes therefore comprise smaller minimum SGs.

Consider, as shown on the left-hand side of Fig. 1, the $s$-dependent discrete energy levels of the ground state and the first excited state of one of the TR problem instances considered in this work (see Sec. 4). Physical intuition suggests that there are regions with a large gap between the two states, where the annealing process can proceed more rapidly without the encountering level transitions. Conversely, in regions characterised by a small SG, the annealing process must conducted at a slower rate to prevent the system from entering higher energy states, as this would result in sub-optimal or invalid solutions. The minimum SG is observed at around $s = 0.85$ and persists at low levels until $s = 1$.

The annealing schedule, denoted by $f(t)$, can be adapted to accommodate the properties of the problem under consideration. Intuitively, this means that during the first three-quarters of the time, the transition from Hamiltonian $\hat{H}_0$ to $\hat{H}_C$ can proceed swiftly, and that it needs to
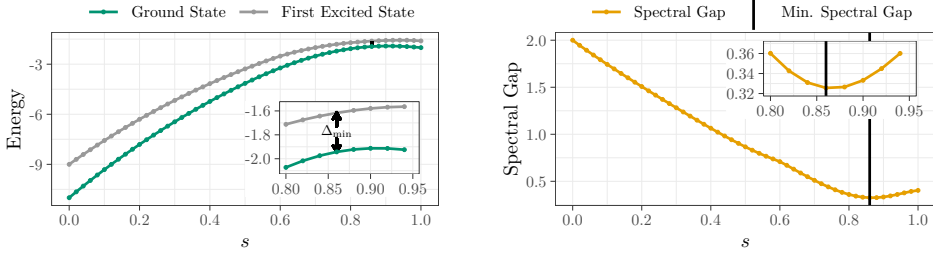
Figure 1: Left: Energy values for ground and first excited state of the Hamiltonian given in Eq. 1 over interpolation parameter $s$ for an example TR problem instance considered in this work. Right: Corresponding SG (*i.e.*, the difference between energy levels of the first excited and the ground state). Lines do not provide an interpolation, but are only used to guide the eye; insets magnify the region around the minimal SG.

slow down in the last quarter. However, givent the computational complexity of the energy spectrum of the Hamiltonian (Eq. 1) and its unavailability prior to the problem's formulation, alternative means of determining good schedules are necessary.

## 3 Quantum Approximate Optimisation Algorithm

One such possibility is to use insights gained from QAOA computations. As QA, the QAOA is designed to optimise QUBO problems. It employs a quantum circuit with $p \in \mathbb{N}$ layers of unitary operators defined by $2p$ parameters $\vec{\beta}, \vec{\gamma} \in \mathbb{R}^p$. A QAOA layer $j \in [1, p]$ comprises two unitaries:

$$U_M(\beta_j) = e^{-i\beta_j \hat{H}_M} \quad \text{and} \quad U_C(\gamma_j) = e^{-i\gamma_j \hat{H}_C} \tag{2}$$

with $U_M$ representing mixer Hamiltonian $\hat{H}_M$, and $U_C$ based on the cost Hamiltonian $\hat{H}_C$, of which the ground state encodes the optimal solution to a given QUBO problem. The mixer unitary $U_M$ typically consists of $\hat{X}$-rotations of size $\beta_j$ on each qubit, while the cost unitary $U_C$ uses single, or multi-qubit $\hat{Z}$-rotations of size $\gamma_j$. The initial state $|s\rangle$ of the QAOA algorithm is usually chosen as the ground state of $H_M$, in which each qubit is in an equal superposition of $|0\rangle$ and $|1\rangle$, prepared using a layer of Hadamard gates. The repeated application of these layers results in the parameterised quantum state

$$|\gamma, \beta\rangle = U_M(\beta_p)U_C(\gamma_p)\cdots U_M(\beta_1)U_C(\gamma_1)|s\rangle, \tag{3}$$

which corresponds to the discretised time evolution governed by the Hamiltonians $H_M$ and $H_C$. A general example of a three-qubit QAOA circuit with $p = 2$ is illustrated in Fig. 2. It has been established that the quality of the approximation increases for a larger number of layers [15]. However, it is important to note that the overall solution quality is significantly influenced by the parameter values $\vec{\beta}$ and $\vec{\gamma}$.
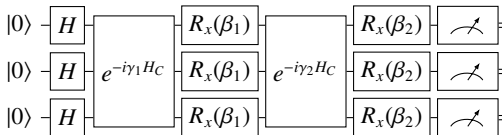


Figure 2: QAOA circuit for cost Hamiltonian $H_C$ and parameter vectors $\vec{\beta}$, $\vec{\gamma}$ of size $p = 2$.

### 3.1 Annealing Schedule Derivation

It is known [9] that the optimal parameter vectors $(\vec{\gamma}^*, \vec{\beta}^*) = \arg\min_{\vec{\gamma}, \vec{\beta}} \langle \vec{\gamma}, \vec{\beta} | H_C | \vec{\gamma}, \vec{\beta} \rangle$, where $\langle \vec{\gamma}, \vec{\beta} | H_C | \vec{\gamma}, \vec{\beta} \rangle$ is the observed mean energy of the final quantum state, can be interpreted as (smooth) annealing path with total annealing time given by $T = \sum_{i=1}^{p}(|\gamma_i^*| + |\beta_i^*|)$. The path itself is constructed from supporting points $f(t_i) = \frac{\gamma_i^*}{|\gamma_i^*| + |\beta_i^*|}$ that are connected via linear interpolation, with time $t_i$ chosen as the mid-point of interval $\gamma_i^*, \beta_i^*$. However, finding *optimal* parameters $\vec{\gamma}^*, \vec{\beta}^*$ is shown to be **NP**-hard [16], albeit for smaller depths, empirical and theoretical results ascertain that optimal values can be well approximated for many subject problems [17].

### 3.2 Structure of the QAOA parameter space

In order to ascertain the optimal parameters, there are several approaches that may be adopted. Firstly, there is the possibility of inspiration by adiabatic time-evolution as evidenced in the works of [9, 18]. Secondly, there is the option of utilising classical optimisation routines [19, 20], where parameter vectors $\vec{\gamma}, \vec{\beta}$ are obtained via an iterative quantum-classical scheme. In the standard formulation of QAOA, the depth $p$ is selected in advance. In essence, larger values of $p$ yield monotonically improving solution quality on perfect hardware. However, for noisy systems, a trade-off exists between enhanced solution quality and an escalating amount of noise and imperfections caused by deeper circuits with growing $p$ which has to be taken into account. In the simplest case, the initial set of values for $\vec{\gamma}, \vec{\beta}$ may be chosen randomly, although more informed choices are possible (see, *e.g.*, [21]).

The FOURIER strategy introduced by Zhou *et al.* [9] comprises two heuristic improvements to the basic scheme: (1) By executing multiple runs of the algorithm iteratively with growing values for $p$, good initial estimates for $\vec{\gamma}, \vec{\beta}$ are determined. The optimal parameters obtained in run $p$ are used to provide suitable initial values for the deeper circuit $p + 1$. (2) To reduce the effective dimension of the parameter space, the set of $2p$ parameters $(\vec{\gamma}, \vec{\beta}) \in \mathbb{R}^{2p}$ is replaced by a new set $(\vec{u}, \vec{v}) \in \mathbb{R}^{2q}$ with $q \leq p$ so that each of the elements $\gamma_i, \beta_i$ of the former set (with $i \in [0, p-1]$) can be expressed as a discrete sine/cosine transform of the set $\vec{u}, \vec{v}$. By choosing a specific value of $q$, the dimension of the effective optimisation parameter space can be delimited at will, at the possible expense of solution quality, but also a reduced complexity of the classical optimisation sub-task of QAOA.

## 4 Methodology

In this work, we address the **NP** problem of Track Reconstruction (TR), a key computing challenge in NHEP. While several classical heuristic methods [22, 23] have been proposed to recognise tracks in the event data of the Large Hadron Collider (LHC), recent publications also approach this problem from the perspective of quantum computing [5, 24], for instance through casting it in QUBO form [8, 25].

The QUBO formulation that is employed in this work is introduced by Bapst *et al.* [8], and also based on the corresponding implementation [1]. While a comprehensive formulation is provided in Ref. [8], the central concept is to reconstruct complete tracks from smaller track segments consisting of three hit-points, referred to as *triplets*. The QUBO is then given by

$$Q(\vec{a}, \vec{b}, \vec{T}) = \sum_{i=1}^{N} a_i T_i + \sum_{i=1}^{N} \sum_{j<i}^{N} b_{ij} T_i T_j, \tag{4}$$

---

[1] github/derlin/hepqpr-qallse

where $\vec{a} \in \mathcal{R}^N$ and $\vec{b} \in \mathcal{R}^{N \times N}$ are constant bias and coupling weights, respectively, and $\vec{T} \in \{0, 1\}^N$ denotes variables for potential triplets.

With growing problem size, the QUBO formulation becomes too large to fit on current quantum systems, requiring one qubit per variable, and therefore also unfeasible to simulate classically. This limitation is particularly evident in the case of full TR, where the number of potential triplets increases rapidly with the complexity of the data. To address this challenge, we adopt a strategy, similar to the approach in Ref. [25], where we only focus on angle segments of a carefully selected data fraction [8] of the hitpoints in the detector for the TR process. This approach also allows to obtain multiple problem instances from the data of one event.

In particular, for our numerical experiments, we filter 10% of the TrackML data [6] for one event, and divided it separately into 32 and 64 angle segments. Additionally, we filtered 20% of data for one event, and obtained 64 angle segments. As we are simulating the quantum systems classically, we discard all QUBOs encompassing more than 23 variables, leading to 98 problem instances in total. While only a part of the tracks can be analysed this way, such reduced problems can act as a proof-of-concept on the potential of QA and QAOA approaches on TR.

# 5 Experimental Results
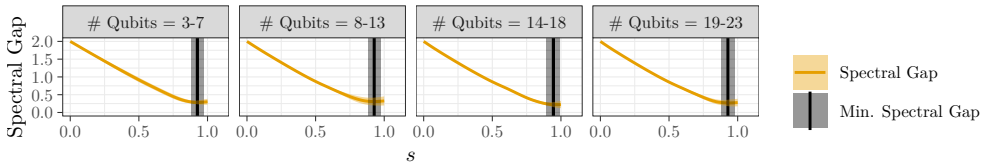
## 5.1 Spectral Gap Analysis



Figure 3: Average SG and the corresponding position of the minimum SG over interpolation parameter $s := t/T$ for 98 TR problem instances with varying sizes. In each qubit range we computed SGs for $20 \ldots 30$ problem instances. Shaded areas represent the standard deviation.

As described in Sec. 2, the SG gives an indication of the required runtime of an algorithm. For the TR instances considered in this work, we obtain the SGs of the interpolation from $\hat{H}_0$ to $\hat{H}_C$ by analytically computing the eigenvalues of Eq. 1 with 50 linearly increasing values of the interpolation factor $s \in [0, 1]$ (*i.e.* at $s = 0$ and $s = 1$, only $\hat{H}_0$ and $\hat{H}_C$ are represented, respectively). As shown in Fig. 3, the average SG does not exhibit significant variation across different qubit numbers, demonstrating a notable consistency. This stability suggests that the system's energy landscape remains relatively predictable and stable as the problem size changes, indicating that annealing schedules relying on these SGs might maintain their performance characteristics regardless of the problem size. This could be advantageous for tasks like TR, where scalability is paramount.

## 5.2 Annealing Schedules from QAOA

Given the similarity of the SGs throughout the considered problem instances, we randomly pick one 11-qubit instance, for which we derive annealing schedules using QAOA as a proof-of-concept. The first two discrete energy levels and the SG for this specific instance are shown in Fig. 1.

As described in Sec. 3.2, we use the Fourier strategy [9] to obtain near-optimal parameters. To this end, we sequentially optimise the set of Fourier parameters $(\vec{u}, \vec{v}) \in \mathbb{R}^{2q}$ starting from QAOA depth $p = 1$ up to $p = 50$ using the numerical *COBYLA* optimiser [19], and re-use the optimised parameters from each previous depth $p - 1$ as initial values padded with zeros. We employ different values for $q \leq q_{max}$, while $q \leq p$ to limit the number of frequencies in the course of the $(\vec{\beta}, \vec{\gamma}) \in \mathbb{R}^{2p}$ parameters. Additionally, we directly optimise $\vec{\beta}, \vec{\gamma}$, starting from $p = 1$ with a Random Parameter Initialisation (RI), up to $p = 50$, also re-using parameters from the previous depth $p - 1$.

As demonstrated in Fig. 4, the obtained approximation ratios (*i.e.* the ratio between achieved energy and optimal energy) rapidly approach the optimum, when employing the Fourier initialisation. Furthermore, a low-dimensional approximation of the parameter space is sufficient. The use of RI results in relatively lower approximation ratios, which indicates that the Fourier landscape is also easier to optimise classically.
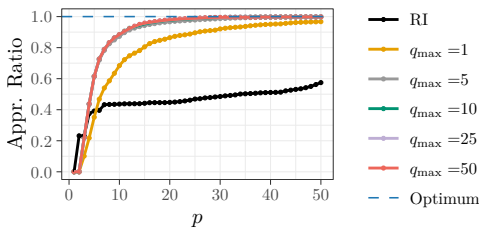


Figure 4: Energy approximation ratio obtained via QAOA optimisation for increasing values of $p$. The approximation ratio curves for $q_{max} \in \{5, 10, 25, 50\}$ exhibit a significant overlap.

Since the parameter vectors $\vec{\gamma}, \vec{\beta}$ can be derived from the effective parameters $\vec{u}, \vec{v}$, it is also possible to derive annealing schedules from these quantities, as described in Sec. 3.1. The derived schedules are shown on the right side of Fig. 5, for the QAOA depth $p = 50$ and varying degrees of approximation (specified by $q_{max}$). The left side of Fig. 5 shows the QAOA parameter vectors $\vec{\gamma}, \vec{\beta}$, which were used for the schedule computation. For RI, the parameter values exhibit significant fluctuations compared to those obtained from the Fourier strategy. However, the corresponding annealing schedule aligns with the intuition gained in Section 2 as annealing progresses rapidly until $s \approx 0.85$, as illustrated by the horizontal line, and subsequently slows down.
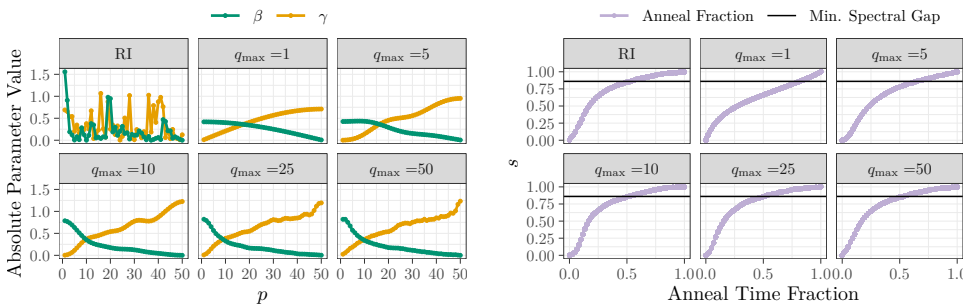


Figure 5: Left: Absolute parameter values $\vec{\beta}$ and $\vec{\gamma}$ obtained from the QAOA optimisation at $p = 50$ for the TR problem instance considered in this work. Right: Annealing schedules obtained from these parameters. The horizontal line denotes the position of the minimal SG.

The Fourier strategy, which achieves near-optimal parameters even with $q_{max} = 5$ (cf. Fig. 4), results in smooth parameter trajectories that produce similar schedules as RI for $q_{max} \geq 5$. Using too few effective Fourier parameters (*i.e.* $q_{max} = 1$) leads to a suboptimal annealing schedule, which is closer to the default linear schedule.

## 6 Discussion & Conclusion

The interplay between QAOA parameters and annealing schedules presents a challenging *chicken-and-egg* problem: Achieving optimal QAOA parameters can inform effective annealing schedules, while simultaneously, annealing motivates QAOA in the first place. This intricate relationship underscores the importance of balancing computational complexity with solution quality, particularly in the context of NISQ computing.

Our analysis has demonstrated that heuristics, such as the FOURIER-based approach proposed in Ref. [9], offer valuable intuition and practical benefits for navigating this complex landscape. By focusing on lower-frequency components in the parameter space, we have shown that it is possible to derive reasonable annealing schedules, reducing resource requirements while maintaining high solution quality. While the implications of these findings and experimental validation of the obtained schedules on quantum annealers such as D-Wave systems extend beyond the specific context of the TR problem, considered in this work, this study suggest promising avenues for generalisation across a wide range of **NP** optimisation problems within NHEP applications. As co-designed quantum algorithms continue to evolve, the development of heuristic methods that bridge the gap between parameter optimisation and annealing schedules will play a pivotal role in unlocking quantum advantage.

The aim of this research is to contribute to a growing understanding of the interplay between QAOA parameters and annealing schedules, as demonstrated on a specific problem in TR. As the field of quantum computing continues to advance, particularly from the NISQ era to fault-tolerance, such investigations will be instrumental in realising the full potential of quantum optimisation techniques to tackle complex, large-scale problems in diverse domains.

## References

[1] M. Franz, P. Zurita, M. Diefenthaler, W. Mauerer, Co-Design of Quantum Hardware and Algorithms in Nuclear and High Energy Physics, EPJ Web of Conferences **295**, 12002 (2024). 10.1051/epjconf/202429512002

[2] J. Preskill, Quantum Computing in the NISQ era and beyond, Quantum **2**, 79 (2018). 10.22331/q-2018-08-06-79

[3] A.I. Pakhomchik, S. Yudin, M.R. Perelshtein, A. Alekseyenko, S. Yarkoni, Solving workflow scheduling problems with QUBO modeling (2022). 10.48550/arXiv.2205.04844

[4] H. Okawa, Q.G. Zeng, X.Z. Tao, M.H. Yung, Quantum-Annealing-Inspired Algorithms for Track Reconstruction at High-Energy Colliders, Computing and Software for Big Science **8**, 16 (2024). 10.1007/s41781-024-00126-z

[5] A. Zlokapa, A. Anand, J.R. Vlimant, J.M. Duarte, J. Job, D. Lidar, M. Spiropulu, Charged particle tracking with quantum annealing-inspired optimization, Quantum Machine Intelligence **3**, 27 (2021). 10.1007/s42484-021-00054-w

[6] M. Kiehn, S. Amrouche, P. Calafiura, V. Estrade, S. Farrell, C. Germain, V. Gligorov, T. Golling, H. Gray, I. Guyon et al., The trackml high-energy physics tracking challenge on kaggle, EPJ Web of Conferences **214**, 06037 (2019). 10.1051/epjconf/201921406037

[7] T. Albash, D.A. Lidar, Adiabatic quantum computation, Rev. Mod. Phys. **90**, 015002 (2018). 10.1103/RevModPhys.90.015002

[8] F. Bapst, W. Bhimji, P. Calafiura, H. Gray, W. Lavrijsen, L. Linder, A. Smith, A Pattern Recognition Algorithm for Quantum Annealers, Computing and Software for Big Science **4** (2019). 10.1007/s41781-019-0032-5

[9] L. Zhou, S.T. Wang, S. Choi, H. Pichler, M.D. Lukin, Quantum Approximate Optimization Algorithm: Performance, Mechanism, and Implementation on Near-Term Devices, Physical Review X **10**, 021067 (2020). 10.1103/PhysRevX.10.021067

[10] W. Mauerer, S. Scherzinger, 1-2-3 Reproducibility for Quantum Software Experiments, in *IEEE Int. Conf. on SW Analysis, Evolution and Reengineering* (2022), pp. 1247–1248

[11] M. Franz, M. Strobl, Reproduction package for "From hope to heuristic: Realistic runtime estimates for quantum optimisation in NHEP" (2025), https://doi.org/10.5281/zenodo.14921650

[12] A. Javadi-Abhari, M. Treinish, K. Krsulich, C.J. Wood, J. Lishman, J. Gacon, S. Martiel, P.D. Nation, L.S. Bishop, A.W. Cross et al., Quantum computing with Qiskit (2024). 10.48550/arXiv.2405.08810

[13] A. Lucas, Ising formulations of many NP problems, Frontiers in Physics **2** (2014). 10.3389/fphy.2014.00005

[14] D-Wave, D-Wave Advantage Quantum Computer (2025), https://dwavesys.com

[15] E. Farhi, J. Goldstone, S. Gutmann, A Quantum Approximate Optimization Algorithm (2014). 10.48550/arXiv.1411.4028

[16] L. Bittel, M. Kliesch, Training Variational Quantum Algorithms Is NP-Hard, Physical Review Letters **127**, 120502 (2021). 10.1103/PhysRevLett.127.120502

[17] K. Bharti, A. Cervera-Lierta, T.H. Kyaw, T. Haug, S. Alperin-Lea, A. Anand, M. Degroote, H. Heimonen, J.S. Kottmann, T. Menke et al., Noisy intermediate-scale quantum algorithms, Rev. Mod. Phys. **94**, 015004 (2022). 10.1103/RevModPhys.94.015004

[18] J.A. Montanez-Barrera, K. Michielsen, Towards a universal QAOA protocol: Evidence of a scaling advantage in solving some combinatorial optimization problems (2024). 10.48550/arXiv.2405.09169

[19] M.J.D. Powell, A Direct Search Optimization Method That Models the Objective and Constraint Functions by Linear Interpolation (1994), ISBN 978-90-481-4358-0 978-94-015-8330-5, http://link.springer.com/10.1007/978-94-015-8330-5_4

[20] M. Periyasamy, A. Plinge, C. Mutschler, D.D. Scherer, W. Mauerer, Guided-SPSA: Simultaneous Perturbation Stochastic Approximation Assisted by the Parameter Shift Rule, in *IEEE Int. Conf. on Quantum Computing and Engineering* (2024), Vol. 01, pp. 1504–1515

[21] D.J. Egger, J. Mareček, S. Woerner, Warm-starting quantum optimization, Quantum **5**, 479 (2021). 10.22331/q-2021-06-17-479

[22] ATLAS Collaboration, Fast Track Reconstruction for HL-LHC (2019).

[23] A. Bocci, M. Kortelainen, V. Innocente, F. Pantaleo, M. Rovere, Heterogeneous reconstruction of tracks and primary vertices with the CMS pixel tracker (2020). 10.48550/arXiv.2008.13461

[24] C. Tüysüz, F. Carminati, B. Demirköz, D. Dobos, F. Fracas, K. Novotny, K. Potamianos, S. Vallecorsa, J.R. Vlimant, Particle Track Reconstruction with Quantum Algorithms, EPJ Web of Conferences **245**, 09013 (2020). 10.1051/epjconf/202024509013

[25] T. Schwägerl, C. Issever, K. Jansen, T.J. Khoo, S. Kühn, C. Tüysüz, H. Weber, Particle track reconstruction with noisy intermediate-scale quantum computers (2023). 10.48550/arXiv.2303.13249